



Article

The Effect of Interlayer Materials on the Joint Properties of Diffusion-Bonded Aluminium and Magnesium

Stefan Habisch ^{1,*}, Marcus Böhme ² , Siegfried Peter ³, Thomas Grund ² and Peter Mayr ¹ 

¹ Institute of Joining and Assembly, Chemnitz University of Technology, D-09107 Chemnitz, Germany; peter.mayr@mb.tu-chemnitz.de

² Institute of Materials Science and Engineering, Chemnitz University of Technology, D-09107 Chemnitz, Germany; marcus.boehme@mb.tu-chemnitz.de (M.B.); thomas.grund@mb.tu-chemnitz.de (T.G.)

³ Institute of Physics, Chemnitz University of Technology, D-09107 Chemnitz, Germany; s.peter@physik.tu-chemnitz.de

* Correspondence: stefan.habisch@mb.tu-chemnitz.de; Tel.: +49-371-53132336

Received: 15 December 2017; Accepted: 12 February 2018; Published: 17 February 2018

Abstract: Diffusion bonding is a well-known technology for a wide range of advanced joining applications, due to the possibility of bonding different materials within a defined temperature-time-contact pressure regime in solid state. For this study, aluminium alloys AA 6060, AA 6082, AA 7020, AA 7075 and magnesium alloy AZ 31 B are used to produce dissimilar metal joints. Titanium and silver were investigated as interlayer materials. SEM and EDXS-analysis, micro-hardness measurements and tensile testing were carried out to examine the influence of the interlayers on the diffusion zone microstructures and to characterize the joint properties. The results showed that the highest joint strength of 48 N/mm² was reached using an aluminium alloy of the 6000 series with a titanium interlayer. For both interlayer materials, intermetallic Al-Mg compounds were still formed, but the width and the level of hardness across the diffusion zone was significantly reduced compared to Al-Mg joints without interlayer.

Keywords: diffusion bonding; aluminum; magnesium; interlayer; titanium; silver; PVD-coating; microstructure; tensile testing; fracture surface analysis

1. Introduction

Diffusion bonding is a widely used technology for creating similar and dissimilar joints from challenging materials. These materials are usually joined at elevated temperatures, between 0.5 and 0.8 of the absolute melting point, using a defined contact pressure with a joining time ranging from a few minutes to a few hours. However, the joining process and weldability are highly influenced by the tendency to form oxide layers, e.g., for aluminium and magnesium [1,2]. To improve the limited weldability of aluminium and magnesium, surface treatment is necessary to remove the stable and tenacious oxide layer and limit the formation of brittle intermetallic Al-Mg compounds [3,4].

Diffusion bonding of aluminium and magnesium with interlayer materials has been extensively investigated to improve the joint properties and promote atomic diffusion processes across the bond line [1,3–10]. For this purpose, a large group of interlayer metals is available to influence the properties of the diffusion zone.

Nickel with a thickness of 6 µm was used as interlayer for diffusion bonding of pure aluminium and pure magnesium. After mechanical surface treatment by grinding, both materials were bonded at 440 °C, 1 N/mm² contact pressure and 60 min bonding time. The results showed that the formation of the intermetallic Al-Mg compound can be avoided, but at the interfaces of both aluminium/nickel

and nickel/magnesium, brittle intermetallic compounds were formed. Therefore, a relatively low joint strength of 26 N/mm² was achieved [5].

Good results were achieved for a diffusion bond between AA 6061 and AZ 31 B with zinc or a zinc-aluminium interlayer with a thickness of 35 µm. A shear strength of 86 N/mm² was reached, due to the eutectic formation of Al-Zn compounds along the bond line. No formation of intermetallic Al-Mg compounds was observed, but intermetallic Mg-Zn compounds still limited the joint strength [6,7].

Silver as interlayer material was examined for diffusion bonds of pure aluminium to pure magnesium. The maximum joint strength of 14.5 N/mm² was reached at 390 °C bonding temperature, 30 min holding time and 5 N/mm² contact pressure with a silver layer thickness of 25 µm. The silver diffused completely into both base materials, and brittle intermetallic compounds of Al-Mg and Mg-Ag were formed. Furthermore, the hardness measurement across the diffusion zone revealed a hardness peak on the magnesium side of the diffusion zone, which consisted of different Mg-Ag phases and weakened the joint [8,9].

The aim of this investigation was to systematically study the effect of titanium and silver as interlayer materials on microstructure and mechanical properties for different Al-Mg diffusion bonds.

2. Experimental Section

2.1. Materials, Equipment and Process Parameters

For this study, the aluminium alloys AA 6060, AA 6082, AA 7020 and AA 7075 and the magnesium alloy AZ 31 B were investigated. The chemical composition of the materials is summarized in Table 1. All aluminium alloys were used in the T6 heat-treated condition except for AA 6060, which was used in condition T66.

Table 1. Chemical composition of the base materials according to manufacturer's specifications [11,12].

Materials	Chemical Composition in wt %								
	Al	Mg	Zn	Si	Cu	Mn	Fe	Ti	Cr
AA 6060	bal.	0.35–0.6	0.15	0.3–0.6	0.1	0.1	0.1–0.3	0.1	0.05
AA 6082	bal.	0.6–1.2	0.2	0.7–1.3	0.1	0.4–1.0	0.5	0.1	0.25
AA 7020	bal.	1.0–1.4	4.0–5.0	0.35	0.2	0.05–0.5	0.4	-	0.1–0.35
AA 7075	bal.	2.1–2.9	5.1–6.1	0.4	1.2–2.0	0.3	0.5	0.2	0.18–0.28
AZ 31 B	2.8–3.0	bal.	1.0	-	-	-	-	-	-

Cylindrical specimens 20 mm in diameter and 15 mm in length for the aluminium alloys and 10 mm in length for the magnesium alloy were machined. Aluminium samples were produced by turning. The magnesium samples were cut out of sheet metal using a water jet. The joining surfaces were therefore equivalent to the rolled surfaces of the sheets.

All surfaces were characterized by tactile surface measurement (Hommel Etamic T8000, Jenoptic, Jena, Germany). An area of 1.5 mm by 1.5 mm was measured with a tip radius of 5 µm and 90° angle (measuring sensor: Hommel Etamic TKL 100, Jenoptic, Jena, Germany) and a measuring speed of 0.15 mm/s.

Joining was carried out using a PVA TePla COV 323 HP diffusion bonding machine (PVA TePla AG, Wettengel, Germany) directly coupled to a glovebox. Details of the setup can be seen in Figure 1 and in [13]. Bonding temperatures of max. 1100 °C and loads of max. 100 N/mm² for an area of 300 mm by 300 mm. Diffusion bonding experiments were carried out under argon with a pressure of 700 hPa. A bonding temperature of 415 °C, bonding time of 60 min and a contact pressure of 8.5 N/mm² was used, based on preliminary experiments on aluminium and magnesium diffusion bonding. All bonding parameters, such as temperature, time and pressure, were automatically controlled throughout the whole bonding process. For each configuration, six specimens were bonded. One specimen was

subjected to a detailed metallographic investigation and micro hardness measurements and five specimens were used for tensile testing. The bonded samples were machined to top hat samples (Figure 2a), in accordance with the ram tensile test [14]. The tensile strength was determined using a universal test machine and a special punch-die-equipment (Figure 2b). Fracture surfaces of tensile specimens and the microstructural characteristics of the diffusion zone were examined using a SEM (Zeiss LEO1455VP, Carl Zeiss AG, Oberkochen, Germany) and EDXS analysis (EDAX Genesis, AMETEK, Inc., Berwyn, PA, USA).

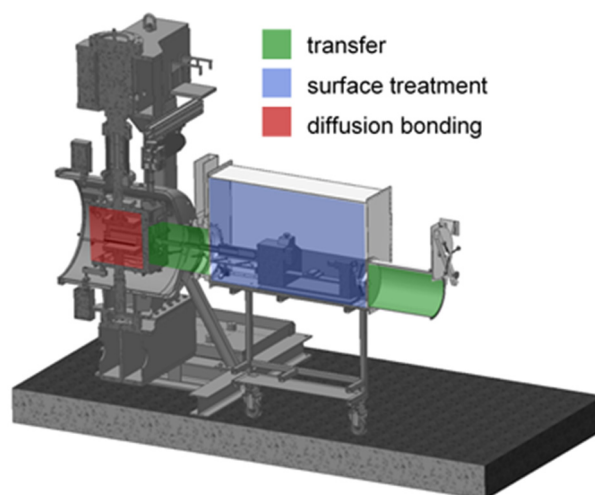


Figure 1. Sectional view of the technology for in-line surface treatment and diffusion bonding.

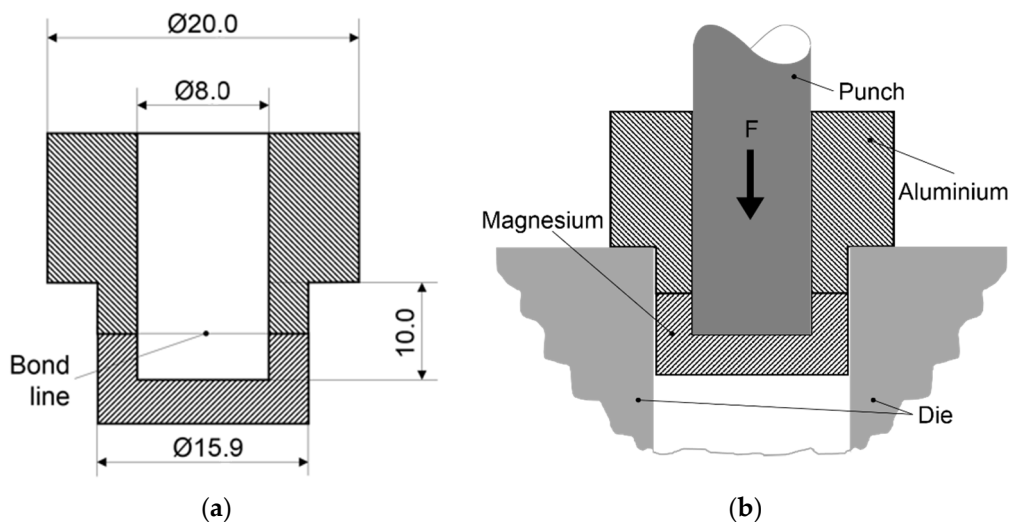


Figure 2. Tensile testing of diffusion bonded joints (a) characteristic geometrical dimensions of a top hat sample and (b) schematic testing setup.

2.2. Surface Preparation

All aluminium samples were machined to a pre-defined surface roughness. Subsequently, the joining surfaces were cleaned using an electron beam and immediately coated with titanium or silver using physical vapor deposition (PVD). The layer thickness for all layers was 2 μm . Therefore, the new formation of oxide layers on the joining surfaces was inhibited. Titanium was chosen as interlayer because the interlayer will form a diffusion barrier for the intermetallic Al-Mg compounds during diffusion bonding. However, the interdiffusion of Al-Ti and Mg-Ti will form the joint between

the aluminum and magnesium materials. In contrast to titanium, silver shows a good diffusivity of Al-Ag and Mg-Ag. The diffusion of silver into the base materials can influence the interface properties most-likely. Furthermore, the soft silver interlayer will improve the forming process of the joining surfaces to each other.

The magnesium surfaces were chemically treated in the glovebox directly before joining. The oxide layer was removed by immersing the specimens in HNO_3 with a chemical concentration of 10 wt % for 30 s. Both the titanium and silver coatings and the chemical surface treatment were carried out so that the roughness of the joining surfaces was not significantly affected.

2.3. Diffusion Bonding Procedure

After the chemical surface treatment, the aluminium and magnesium samples were assembled on top of each other and transferred from the glovebox into the diffusion bonding chamber. A small contact pressure of ca. 3 N/mm^2 was applied during heating up to 350°C (heating rate of $3\text{--}5 \text{ K min}^{-1}$), to reduce the macroscopic deformation of the magnesium sample. When a temperature of 350°C was reached, the contact pressure was increased to 8.5 N/mm^2 to reach a near full-faced contact. At 415°C , the pre-determined bonding time of 1 h was held. At the end of the diffusion bonding procedure, specimens were cooled to room temperature in the chamber at $2\text{--}10 \text{ K min}^{-1}$.

3. Results and Discussion

3.1. Joining Surfaces

The surface roughness S_z after turning of the aluminum specimens was $S_z = 5.2 \mu\text{m} \pm 0.3 \mu\text{m}$. Coating only slightly changed the joining surfaces to $S_z = 5.1 \mu\text{m} \pm 0.2 \mu\text{m}$. The macroscopic characteristic traces of the turning process were still visible (Figure 3a). The chemical surface treatment of AZ 31 B changed the surface roughness from $S_z = 21.6 \mu\text{m}$ to $S_z = 20.4 \mu\text{m}$, due to the removal of material (Figure 3b).

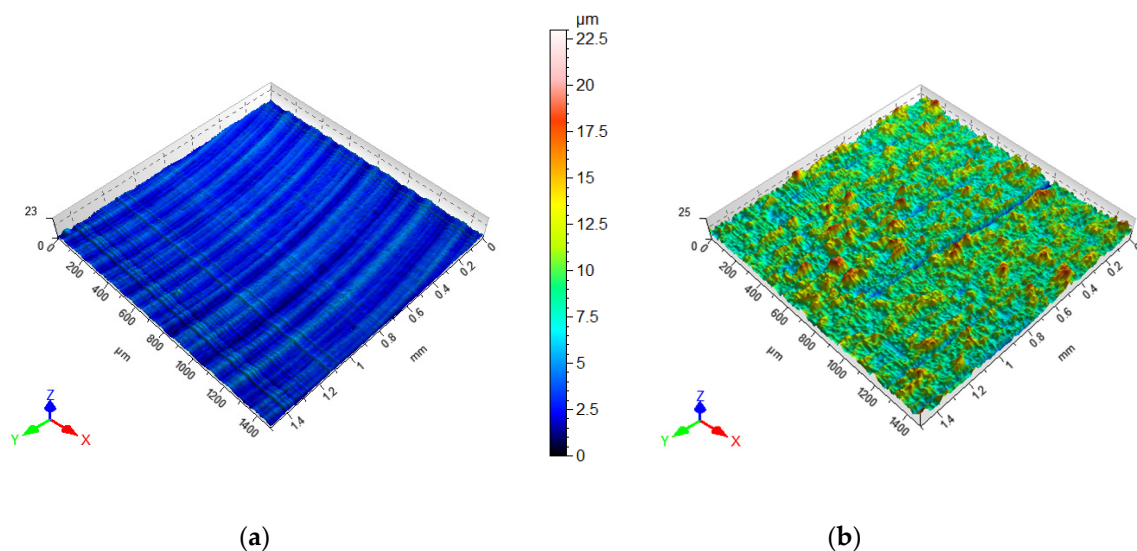


Figure 3. Tactile measured surface topographies of the joining surfaces after surface treatment with (a) $S_z = 5.2 \mu\text{m}$ of AA 6082 coated with titanium and (b) $S_z = 20.4 \mu\text{m}$ of AZ 31 B after chemical treatment.

The rolled magnesium surfaces exhibit a higher surface roughness compared to the aluminium surfaces, but through the enhanced formability of AZ 31 B above 230°C , a full-faced contact can be assumed. Furthermore, through a higher surface deformation, the amount of lattice defects increases, and thus diffusivity is enhanced.

3.2. Joint Properties with Titanium Interlayer

All aluminium alloys showed a similar morphology in the diffusion zone. Figure 4 depicts the diffusion zone of an AA 7020-AZ 31 B bond. No diffusion of titanium into the aluminium was detected. The interlayer showed similar thickness to the as-coated condition with the exception that a few discontinuities due to fracture of the layer were observed. The EDXS line scan confirmed the interdiffusion of Al and Mg for all joints. Mg, in particular, diffused from the AZ 31 B into the base materials of the 6000 series aluminum alloys, and Al-Mg compounds were formed. The aluminium alloys of the 7000 series showed a higher concentration of Zn in the diffusion zone and intermetallic Al-Mg compounds, respectively (Figure 5). Characterization confirmed that the formation of the intermetallic Al-Mg compound was not avoided by the titanium interlayer. The discontinuous layer structure and the relatively thin layer thickness most likely were not sufficient to suppress interdiffusion. The thickness of ca. 40–50 μm of the intermetallic Al-Mg compound along the interface is similar to the results of joining experiments without interlayer material for the same bonding parameters, e.g., compared to the results of Dietrich et al. [15]. However, no joints with titanium interlayer exhibited cracks or voids along the bond interface, indicating that full metallic continuity had been reached.

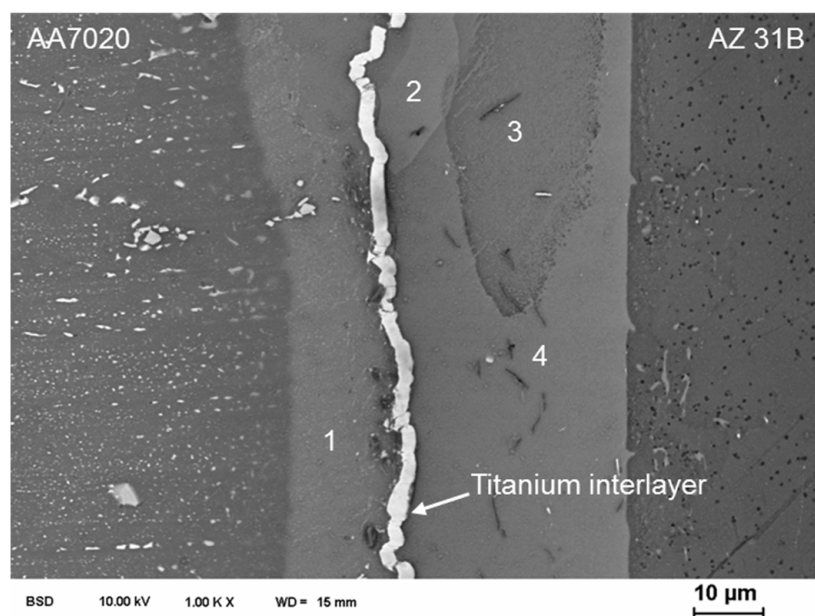


Figure 4. SEM image of the diffusion zone of Al-Mg joint consisting of (1) Al_3Mg_2 ; (2) $\text{Al}_{12}\text{Mg}_{17}$ with ca. 3 at-% Zn; (3) $\text{Al}_{12}\text{Mg}_{17}$ with ca. 2 at-% Zn; and (4) $\text{Al}_{12}\text{Mg}_{17}$.

Figure 6 shows the results of Vickers micro-hardness measurements across the interface of the Al-Mg joints. A significant increase in hardness can be seen for all diffusion zones of the bonds. The magnesium side of the 7000 series aluminium joints show a different behavior compared to the 6000 series. The correlation of Figures 5 and 6 confirms that a higher concentration of zinc on the magnesium side leads to higher micro-hardness.

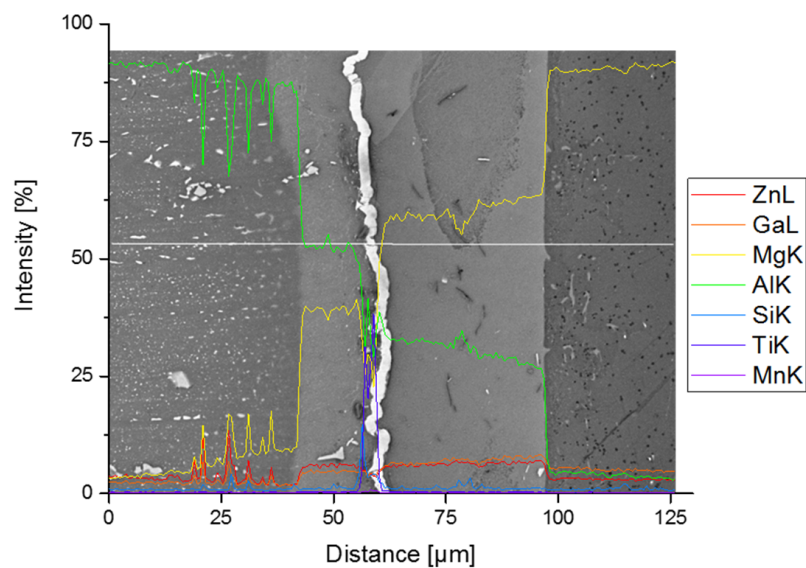


Figure 5. Elemental distribution across the interface of the Al-Mg joint of with titanium interlayer (Figure 4) measured by EDXS line scan.

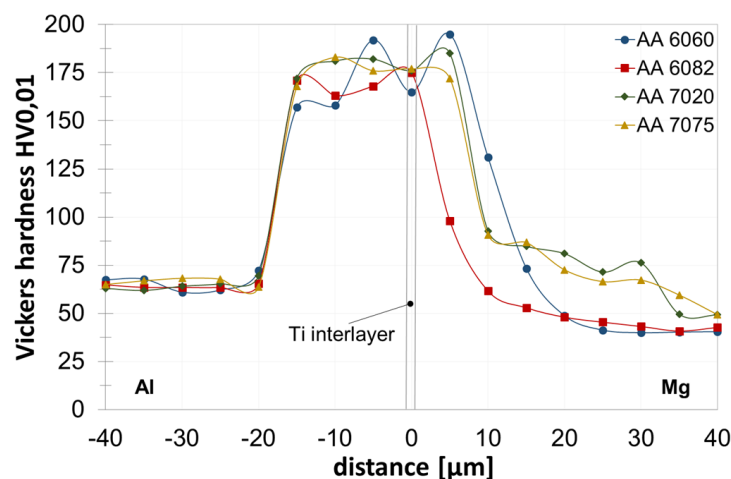


Figure 6. Hardness profiles across the interface of the diffusion-bonded Al-Mg joints with titanium interlayer.

3.3. Joint Properties with Silver Interlayer

In contrast to the results with titanium interlayer, a reaction of the silver coating with the base materials during joining was observed. The silver diffused completely into the base materials, and an intermetallic Al-Mg compound was formed. This zone also contained silver. The white dotted regions in zone 3 of Figure 7 are slightly enriched in silver (Figure 8). Kirkendall voids were formed on the magnesium side, due to the higher coefficient of diffusion of magnesium atoms in aluminium. This is in accordance with other researchers, such as Jafarian et al. [10], who observed similar phenomena for diffusion bonding of aluminium and magnesium with or without interlayer materials. An increase in the contact pressure will avoid the formation of Kirkendall voids; however, macroscopic deformation will increase. The hardness profiles of the Al-Mg joints with silver interlayer exhibit an increase in hardness at the interface of the intermetallic compound $\text{Al}_{12}\text{Mg}_{17}$ and the magnesium base material. This is pronounced for the aluminum alloys of the 7000 series (Figure 9). The chemical composition of the areas of high hardness again showed an increase of zinc in this area. The enrichment of zinc in the magnesium can form a metallurgical notch in this area away from the bond line. This notch effect is a

typical cause of failure for similar and dissimilar joints. For aluminium and magnesium joints without interlayer, the metallurgical notch is located at the interface of the aluminium base material and the Al_3Mg_2 intermetallic compound. These effects were also observed by Liu et al. [7,10].

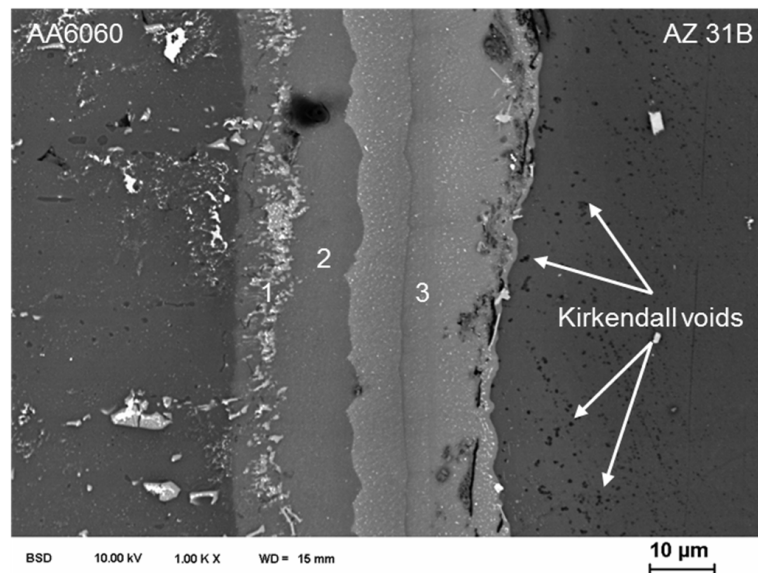


Figure 7. SEM image of the diffusion zone of an Al-Mg joint revealing (1) impurities of Al, Mg, Si and O_2 , (2) the Al-rich intermetallic phase Al_3Mg_2 with ca. 1.5 at-% Ag and (3) the Mg-rich intermetallic phase $\text{Al}_{12}\text{Mg}_{17}$ with ca. 3 at-% Ag.

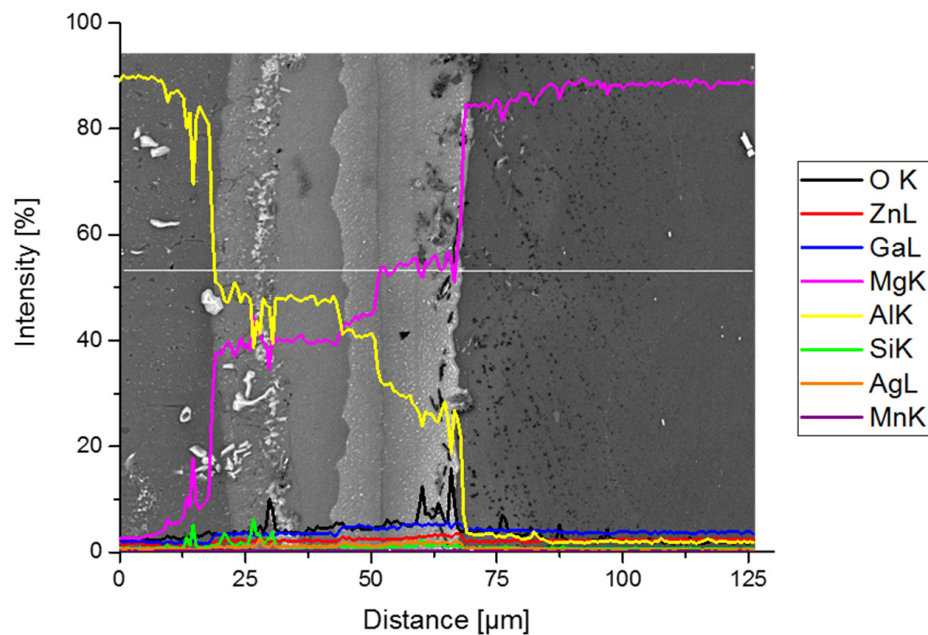


Figure 8. Elemental distribution across the interface of the Al-Mg joint with silver interlayer (Figure 6) measured by EDXS line scan.

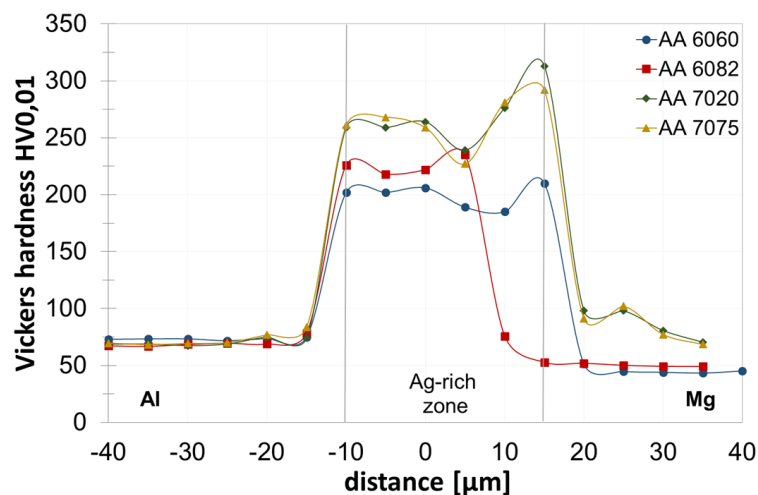


Figure 9. Hardness profiles across the interface of the diffusion-bonded Al-Mg joints with silver interlayer.

3.4. Tensile Testing and Fractography

Figure 10 summarizes the results of the tensile tests with the top hat specimens. Joints with titanium interlayer exhibit the highest strength levels, especially for the aluminium alloys of the 6000 series. The hardness measurements of these show the lowest increase in hardness across the diffusion zone. The hardness profiles of the 7000 series aluminium alloys show an increased hardness by 75 HV 0.01. The fracture surface of an AA 6060 and AZ 31 B joint shows a dense layer of the titanium coating with only few areas of intermetallic Al-Mg compounds (Figure 11). For both the AA 6060 and the AA 6082 aluminium alloys, the fracture surfaces exhibited a dense titanium coating that corresponds to the high rupture strength of 48.3 N/mm². However, lower joint strengths were observed for the 7000 series joints with titanium interlayer. The fracture surfaces of the AA 7020 reveals a higher amount of intermetallic Al-Mg compounds (Figure 12). These intermetallic compounds exhibit very brittle behavior, especially when exposed to a tensile load. As a consequence, the base material strength of magnesium of 260 N/mm² was not nearly reached. Furthermore, a partial delamination of the titanium coating was observed on the fracture surfaces (Figure 12, No. 3). Significant lower joint strengths were achieved using silver as interlayer material. The hardness profiles (Figure 8) already showed both a higher averaged hardness level in the diffusion zones and a hardness peak on the magnesium side of the 7000 series aluminium alloys. The fracture surface of the aluminium side, shown in Figure 13, exhibits a rough surface, which is characteristic of brittle failures of intermetallic compounds. The EDXS analysis of the fracture surfaces showed that Al₃Mg₂ and Al₁₂Mg₁₇ intermetallic phases are present. Despite high hardness on the magnesium side and the confirmed metallurgical notch in this position, the joint finally failed in-between the intermetallic compounds. As a result, the rupture strength for AA 7020 was only 27.7 N/mm². In contrast to the 6000 series aluminium alloys (Figure 13), the fracture surface of AA 7020 (Figure 14) appears smoother, but still contains rough areas. The fracture location was probably between the aluminium base material and the intermetallic Al-Mg compound, which contained traces of silver and zinc. Similar fractures as for AA 6060 were observed for AA 6082 and AA 7075.

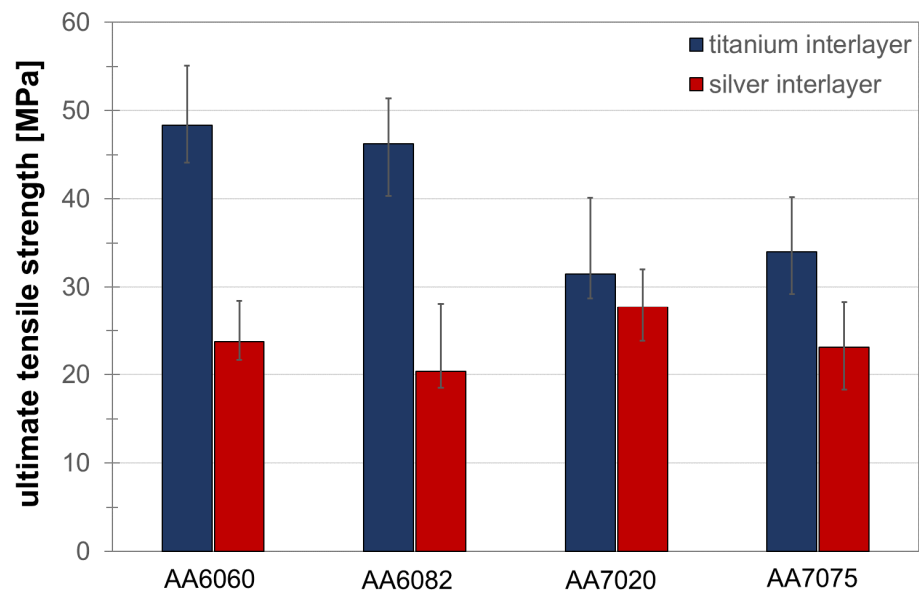


Figure 10. Joint strength of diffusion-bonded aluminum and magnesium with titanium or silver interlayers.

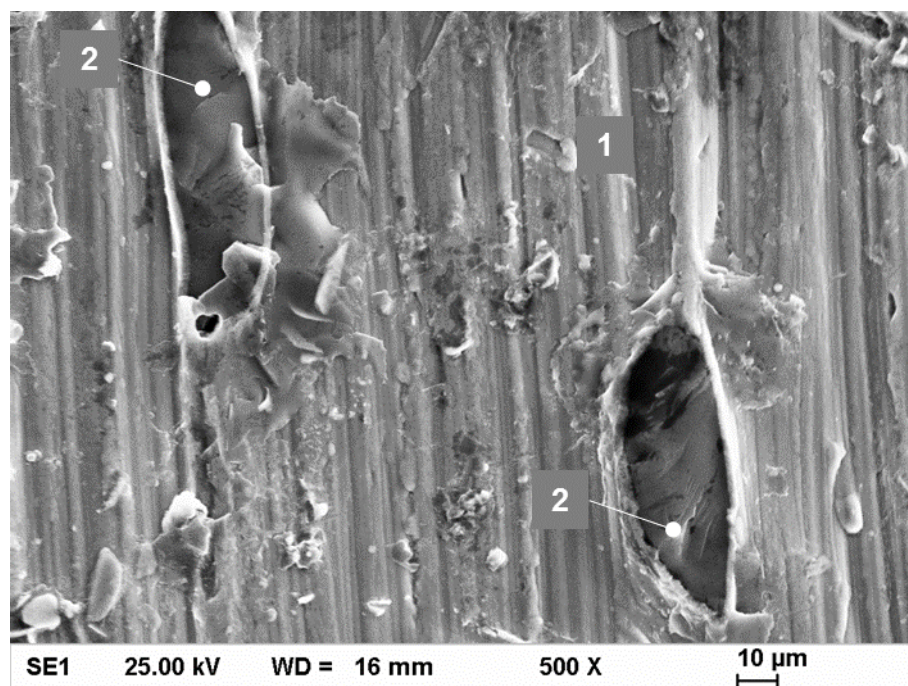


Figure 11. SEM image of a fracture surface of an AA 6060 and AZ 31B joint with titanium interlayer on the aluminium side revealing (1) the surface of the titanium coating with only a few areas of (2) intermetallic Al-Mg compounds.

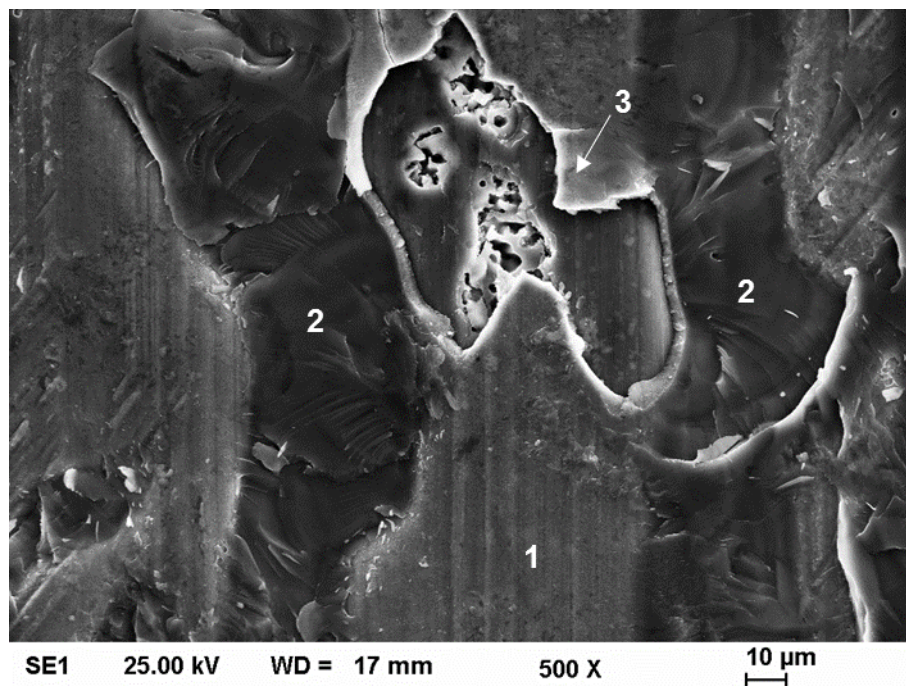


Figure 12. SEM image of a fracture surface of a AA 7020 and AZ 31B joint with titanium interlayer on the aluminium side and (1) the surface of the titanium coating, (2) intermetallic Al-Mg compounds and (3) a delamination of the coating from the aluminium surface.

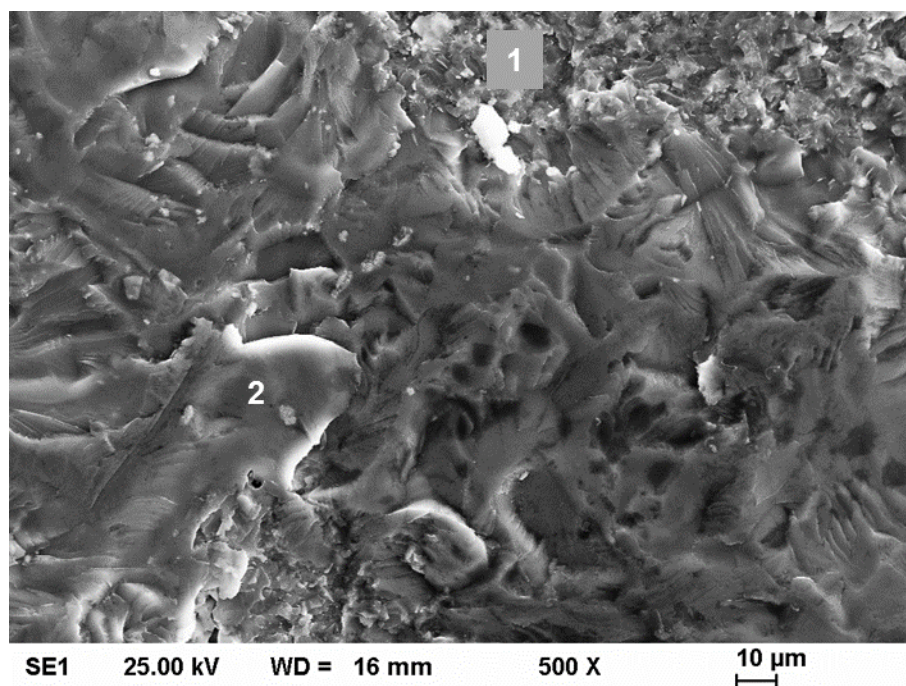


Figure 13. SEM image of a fracture surface of a AA 6060 and AZ 31B joint with silver interlayer on the aluminum side (1) presumably Al_3Mg_2 containing traces of silver and (2) presumably $\text{Al}_{12}\text{Mg}_{17}$ containing traces of silver.

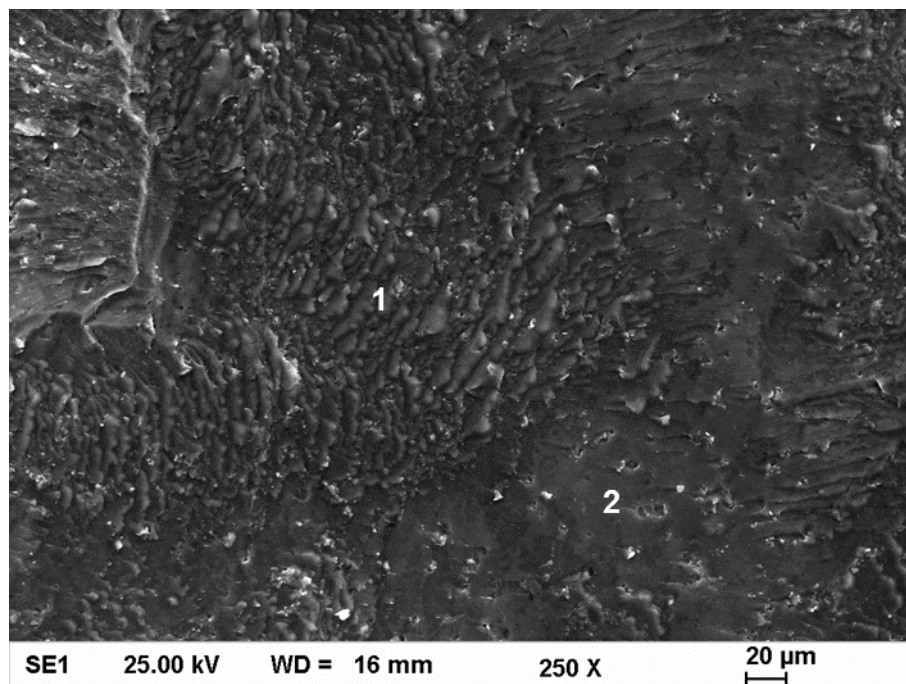


Figure 14. SEM image of a fracture surface of a AA 7020 and AZ 31B joint with silver interlayer on the aluminium side (1) presumably Al_3Mg_2 containing traces of silver and zinc and (2) aluminium base material with traces of magnesium.

4. Conclusions

In the present study, the effect of titanium and silver as interlayer materials on diffusion-bonded AA 6060, AA 6082, AA 7020, AA 7075 and AZ 31 B dissimilar joints was examined. The following conclusions can be derived:

Titanium and silver as interlayers, deposited by a PVD-process on the oxide-free aluminum surface, made redundant a further surface treatment after exposure of specimens to air.

A solid and almost dense interlayer was formed by titanium on the surface. However, intermetallic Al-Mg compounds were still formed during diffusion bonding. Nevertheless, the hardness measurements across the interface showed a lower hardness level for the diffusion zone compared to Al-Mg joints without interlayers. As a consequence, a joint strength of up to 48 N/mm^2 was reached.

The $2 \mu\text{m}$ thick silver interlayer completely diffused into both base materials and formed a brittle diffusion zone. Kirkendall voids were observed on the magnesium side and a joint strength of only 28 N/mm^2 was achieved.

Fracture of the joints with titanium interlayer occurred at the interface of the intermetallic Al-Mg compound and the titanium. As the silver diffused into the base materials, the joints failed at the interface of Al_3Mg_2 and $\text{Al}_{12}\text{Mg}_{17}$.

Acknowledgments: The authors gratefully acknowledge the funding by the German Research Foundation (Deutsche Forschungsgemeinschaft, DFG) within the framework of the Collaborative Research Centre 692 (SFB HALS 692).

Author Contributions: Stefan Habisch carried out all joining experiments and is the main author of this manuscript. Marcus Böhme supported the project with microstructural characterization using SEM and EDS. Siegfried Peter supported the project with the PVD coatings of titanium and silver. Thomas Grund and Peter Mayr are senior scientists, developed and supervised the project “Joining concepts for bulk and sheet metal structures of high-strength light-weight materials” within SFB HALS 692.

Conflicts of Interest: The authors declare no conflict of interest.

References

1. Shirzadi, A.A.; Assadi, H.; Wallach, E.R. Interface evolution and bond strength when diffusion bonding materials with stable oxide films. *Surf. Interface Anal.* **2001**, *31*, 609–618. [CrossRef]
2. Huang, Y.; Humphreys, F.J.; Ridley, N.; Wang, C. Diffusion bonding of hot rolled 7075 aluminium alloy. *Mater. Sci. Technol.* **1998**, *14*, 405–410. [CrossRef]
3. Cherepy, N.J.; Shen, T.H.; Esposito, A.P.; Tillotson, T.M. Characterization of an effective cleaning procedure for aluminum alloys: Surface enhanced Raman spectroscopy and zeta potential analysis. *J. Colloid Interface Sci.* **2005**, *282*, 80–86. [CrossRef] [PubMed]
4. Saleh, H.; Reichelt, S.; Schmidtchen, M.; Schwarz, F.; Kawalla, R.; Krüger, L. Effect of inter-metallic phases on the bonding strength and forming properties of Al/Mg sandwiched composite. *Key Eng. Mater.* **2014**, *622*, 467–475. [CrossRef]
5. Zhang, J.; Luo, G.; Wang, Y.; Shen, Q.; Zhang, L. An investigation on diffusion bonding of aluminium and magnesium using a Ni interlayer. *Mater. Lett.* **2012**, *83*, 189–191. [CrossRef]
6. Liu, L.M.; Zhao, L.M.; Xu, R.Z. Effect of interlayer composition on the microstructure and strength of diffusion bonded Mg/Al joint. *Mater. Des.* **2009**, *30*, 4548–4551. [CrossRef]
7. Liu, L.M.; Zhao, L.M.; Wu, Z.H. Influence of holding time on microstructure and shear strength of Mg–Al alloys joint diffusion bonded with Zn–5Al interlayer. *Mater. Sci. Technol.* **2011**, *27*, 1372–1376. [CrossRef]
8. Wang, Y.; Luo, Q.; Shen, Q.; Wang, C.; Zhang, L. Effect of Holding Time on Microstructure and Mechanical Properties of Diffusion-Bonded Mg1/Pure Ag Foil/1060Al Joints. *Key Eng. Mater.* **2014**, *616*, 280–285. [CrossRef]
9. Wang, Y.; Luo, Q.; Zhang, J.; Shen, Q.; Zhang, L. Microstructure and mechanical properties of diffusion-bonded Mg–Al joints using silver film as interlayer. *Mater. Sci. Eng. A* **2013**, *559*, 868–874. [CrossRef]
10. Jafarian, M.; Khodabandeh, A.; Manafi, S. Evaluation of diffusion welding of 6061 aluminum and AZ31 magnesium alloys without using an interlayer. *Mater. Des.* **2015**, *65*, 160–164. [CrossRef]
11. Magnesium—Otto Fuchs GmbH. Available online: <https://www.otto-fuchs.com/en/competence/materials/magnesium.html> (accessed on 29 November 2017).
12. Bikar Aluminium GmbH. Available online: <http://www.bikar.com/aluminium-round-bars.html> (accessed on 19 January 2018).
13. Mayr, P.; Habisch, S.; Haelsig, A.; Georgi, W. Challenges of joining lightweight materials for dissimilar joints. In Proceedings of the 10th International Conference on Trends in Welding Research and 9th International Welding Symposium of Japan Welding Society (9WS), Tokyo, Japan, 11–14 October 2016.
14. Zatorski, Z. Evaluation of steel clad plate weldability using ram tensile test method. *Mater. Trans.* **2007**, *3*, 229–238.
15. Dietrich, D.; Nickel, D.; Krause, M.; Lampke, T.; Coleman, M.P.; Randle, V. Formation of intermetallic phases in diffusion-welded joints of aluminium and magnesium alloys. *J. Mater. Sci.* **2011**, *46*, 357354. [CrossRef]



© 2018 by the authors. Licensee MDPI, Basel, Switzerland. This article is an open access article distributed under the terms and conditions of the Creative Commons Attribution (CC BY) license (<http://creativecommons.org/licenses/by/4.0/>).